

# Hybrid Cassava Identification from Morphometric Analysis to Deep Convolutional Neural Networks and Confirmation Strategies

Phanupong Changtor<sup>1</sup>, Wachiraphong Ratiphaphongthon<sup>2</sup>, Maturada Saengthong<sup>1</sup>, Kittisak Buddhachat<sup>1,4</sup> and Nonglak Yimtragool<sup>1,3,4,\*</sup>

<sup>1</sup>Department of Biology, Faculty of Science, Naresuan University, Phitsanulok 65000, Thailand

<sup>2</sup>Department of Mathematics, Faculty of Science, Naresuan University, Phitsanulok 65000, Thailand

<sup>3</sup>Center of Excellence for Biodiversity, Faculty of Science, Naresuan University, Phitsanulok 65000, Thailand

<sup>4</sup>Center of Excellence for Innovation and Technology for Detection and Advanced Materials (ITDAM), Naresuan University, Phitsanulok 65000, Thailand

(\*Corresponding author's e-mail: nonglakp@nu.ac.th)

Received: 16 December 2024, Revised: 30 January 2025, Accepted: 6 February 2025, Published: 25 March 2025

## Abstract

The correct identification of cassava varieties is critical for crop management, such as for developing high-value products or against agricultural pests. In this study, plant characteristic regions used for classification were verified by principal component analysis (PCA) techniques. A deep learning method was applied using well-known pretrained models to identify hybrid cassava through image classification. The models employed—ResNet-18, VGG-16, AlexNet, and GoogLeNet—yielded impressive accuracies in three-fold cross-validation experiments, achieving 100, 99.06, 99.06, and 98.59 % averaged accuracy, respectively. The fine-tuned ResNet-18 model had the highest accuracy and was selected for identifying hybrid cassava. A confusion matrix revealed 3 misidentifications. Cultivar variety (cv) R72 was mistakenly classified as R5 in both the 1<sup>st</sup> and 2<sup>nd</sup> folds and as R1 in the 2<sup>nd</sup> fold. Additionally, we utilized Local Interpretable Model-agnostic Explanations (LIME) to ensure that our models offered insightful explanations for their decision-making processes. The outcomes from Principal Component Analysis (PCA) and Local Interpretable Model-agnostic Explanations (LIME) exhibited close resemblance, particularly within the region encompassing the stem, branch, petiole, and stipule of cassava. These findings were leveraged for the identification of the 3 distinct cultivated cassava varieties. The results demonstrated the efficacy of deep learning as a potent technique for discerning hybrid cassava varieties, presenting promising prospects for its practical deployment in on-site testing and widespread adoption due to its time-saving capabilities.

**Keywords:** Cassava, CNN, Deep learning, Fine-tuning, Hybrid identification, LIME, PCA

## Introduction

Cassava, a plant shrub of the Euphorbiaceae family, is a popular food in South America and Southeast Asia, particularly in Thailand and Indonesia. This starchy tuber contains high carbohydrates and calories. Cassava is a drought-tolerant crop that is cultivated in tropical climates but is attacked by a variety of pests that are widespread in tropical areas. Root

destruction is a major issue in agriculture, resulting in loss of production. Several pests such as mealybugs, hornworms, bacteria, and fungi are causative agents for plant disease [1]. Various strategies for pest management control include chemical, biological, and plant resistance cultivation. Pest-resistant plants are a suitable alternative for pest control by demonstrating resistance to infection through structure, preformed chemicals, and plant immune responses. There have been many reports about cassava which is resistant to

some pests such as *Sclerotium rolfsii*, *Phytophthora* spp., *Xanthomonas campestris* pv. *manihotis*, and *Colletotrichum gloeosporioides* f. sp., in which some varieties are hybrid as a result of crossbreeding also demonstrate improved pest-resistant traits [2-4]. In Thailand, several cassava varieties are hybrids of original cultivars created for enhanced ethanol production or tolerance to certain pathogens. Cassava varieties that are resistant to pests include Rayong 5 and Rayong 72 [4]. Thus, the selection of the culture variety is important for cultivation in cassava farming.

The identification of cassava cultivar varieties generally relies on morphological characteristics. Varietal identification with the naked eye may not be able to distinguish cassava variety clearly because the characteristics of leaves and stems are very similar. Nowadays, biomolecular techniques are used to accurately and efficiently differentiate between species based on DNA information. Conventional biomolecular techniques using simple sequence repeat (SSR) molecular markers or microsatellites have been used to identify the various varieties of cassava [5,6]. However, these approaches necessitate the use of costly instrumentation and highly experienced technicians, limiting their suitability for mass use. Morphometric analysis has been trending towards use for identifying cassava culture varieties. There are slight differences in the external appearance of cassava among different cultivated varieties. Computer programs like ImageJ are utilized to identify slight differences in external appearances among different cassava varieties, while ANOVA and PCA are also employed as tools to identify different culture varieties and detect hybrids [7]. However, these techniques are underutilized due to the technical expertise required to operate the software and interpret results. While machine learning techniques have been explored in other crop studies, their application in cassava varietal identification remains underdeveloped. This study applies a deep learning approach to identify 3 cassava cultivated varieties using only image data as input, eliminating the need for costly equipment, complex biomolecular techniques, or specialized software expertise.

Deep learning, a rapidly advancing field of research in machine learning and artificial intelligence (AI), has been extensively employed across various disciplines [8-11]. One powerful technique within deep

learning is transfer learning, where a pretrained neural network model is used as a starting point to solve a different but related task. Instead of training a neural network from the beginning, transfer learning leverages the knowledge gained from solving 1 problem and applies it to a new problem. In the realm of academic research on deep learning, this technique has been particularly beneficial. Recently, transfer learning has been applied in crop management studies including the detection of plant diseases [12-15] or contributing to fruit maturation Saha *et al.* [16] to ensure food security. Recent progress made in image classification opens new possibilities for expanding image processing research and applications in the agricultural field. The agricultural sector has now embraced deep learning and image processing techniques to effectively address the challenges in plant identification. Mehdi-pour Ghazi *et al.* [7] utilized pretrained deep learning models including AlexNet, GoogLeNet, and VGGNet for plant identification. The comparative relative performance showed that GoogLeNet and VGGNet outperformed AlexNet, achieving accuracy rates of 76.87 and 78.44 %, respectively [17]. Similarly, Nguyen *et al.* [18] demonstrated the robustness of deep learning CNNs to automatically identify plant species from flower images using AlexNet, CaffeNet, and GoogLeNet. Their results revealed that GoogLeNet achieved superior performance. By tuning network parameters, the highest performance was observed with an accuracy rate of 67.45 % at rank 1 and 90.82 % at rank 10 [18]. Jasitha *et al.* [19] chose leaves over flowers as a more suitable option for research due to their higher availability, ease of handling, and larger sample size. Moreover, leaves are accessible throughout the year, making them a practical choice for conducting studies. They utilized a fine-tuned GoogLeNet convolutional neural network (CNN) model for plant classification based on leaf venation. Both the GoogLeNet and VGG-16 CNN models were trained and tested using datasets, employing a combination of CNN and Support Vector Machine (SVM) classifiers. Results showed that GoogLeNet surpassed VGG-16, achieving the highest accuracy rate of 99.2 % [19]. Another model, ResNet-18, well-known for its effectiveness, has also been utilized for the precise classification of fruits as excellent or poor by specifically targeting industrial export applications. A ResNet-18 model was trained

using an extensive dataset consisting of fruit images. The results highlighted the model's exceptional performance, achieving a remarkable sensitivity level of 97.46 %. Furthermore, the model also exhibited a substantial precision rate of 98.71 % and a notable F1 parameter value of 98.08 % [20]. In a related study, Arafat *et al.* [21] employed a ResNet-18 model for plant identification based on leaf traits. By training various models utilizing the ResNet-18 architecture, they achieved a notable maximum accuracy of 99 %. Furthermore, when testing the model on a different dataset, they obtained an accuracy rate of 99.9 % [21]. The application of fine-tuning techniques has exhibited a notable level of plant classification accuracy. This approach has also shown promise for the identification of other plant species that have previously received limited attention. The widespread acceptance and practical implementation of conventional machine learning methods have further enhanced agricultural research.

This study aims to develop a tool for mass use to identify hybrid cassava. Principal component analysis (PCA) was used in a preliminary study of probabilistic morphometric characteristics used for hybrid identification, with results utilized to verify the appropriate cassava regions for hybrid identification using deep learning. Several fine-tuned models that utilized different pretrained models were compared including ResNet-18, AlexNet, VGG-16, and GoogLeNet to select the best-performing model based on its target task accuracy. Both accuracy and model size were assessed to strike a balance between performance and resource efficiency. Once the models

were trained, their predictions were evaluated using Local Interpretable Model-agnostic Explanations (LIME) to ensure that the models worked reasonably and provided meaningful explanations for their decisions. LIME is a powerful tool for interpreting black-box machine learning models and generating understandable explanations for individual predictions to gain insights into how the models arrive at their decisions and validate their reasoning [22].

## Materials and methods

### Workflow study for cassava hybrid identification

**Figure 1** illustrates the workflow for hybrid cassava identification, encompassing morphometric analysis, transfer learning, and interpretability using LIME. The process begins with image capture from 3 cassava varieties (where cv R72 is a hybrid of cv R1 and cv R5). These images undergo morphometric analysis, including the measurement of relevant traits using the ImageJ program, statistical assumption checks and PCA for visualization of data distribution. In the transfer learning phase, several pre-trained deep learning models, including ResNet-18, VGG-16, AlexNet, and GoogLeNet, are evaluated. The selected model is then fine-tuned to optimize classification performance across the 3 categories (R1, R5, R72). Finally, interpretability is achieved using LIME. LIME provides visual explanations by highlighting the image regions that contribute most to the classification, enhancing the transparency of model predictions and fostering user trust in the analysis pipeline.

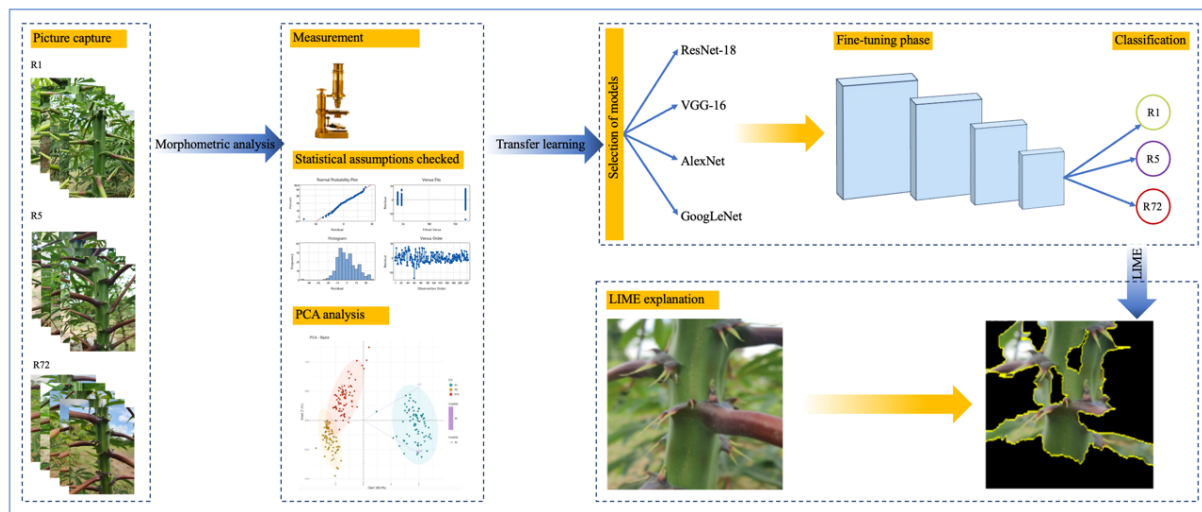


**Figure 1** Conceptual workflow for cassava hybrid identification study.

### Cassava materials and hybrid identification using DNA-based analysis

The cassava cultivars (N=45) Rayong 1 (cv R1), Rayong 5 (cv R5), and Rayong 72 (cv R72) were provided by the Rayong Field Crops Research Center, Rayong, Thailand (**Figure 2**). Each cassava plant was clonally produced from 20 cm long stem cuttings with at least 5 nodes. Plant stems were treated with pesticides Carbendazim:Captan:Metalaxyl at 1:1:1 in 15 L of water for 30 min before planting. Before relocation to the field plot, the plants were planted in plastic bags with a diameter of 8 cm and a height 24 cm using sterile soil and sand at 1:3 for 1 month. DNA extraction was performed using the modified method described by Sharma *et al.* [23] with cassava leaves [23]. Fresh cassava leaves (1 g) were lysed using 500  $\mu$ L of an extraction buffer containing 100 mM Tris pH 8, 10 mM EDTA, 1 % SDS, 2 % PVV, 1 M NaCl, and 1 %  $\beta$ -mercaptoethanol. Then, 100  $\mu$ L of 4 % (w/v) polyethylene glycol (PEG) and 1  $\mu$ L of 25 mg/mL proteinase K were added and the mixture was incubated at 65  $^{\circ}$ C for 1 h. Protein precipitation was then performed using 100  $\mu$ L of 7.5 M ammonium acetate and incubated at 4  $^{\circ}$ C for 30 min. Centrifugation was conducted to remove debris, and the supernatant was mixed with isopropanol (1:1). The mixture was

incubated overnight at  $-20^{\circ}$ C. Subsequently, the tubes were centrifuged for DNA precipitation, and the supernatant was discarded. The DNA was washed with 100  $\mu$ L of 70 % ethanol, followed by centrifugation, air-drying, and resuspension in 20  $\mu$ L of nuclease-free water. The quality and quantity of DNA were measured by Nanodrop (Thermo Scientific<sup>TM</sup>, USA). The DNA obtained was amplified using HotStarTaq DNA Polymerase (Hilden, Germany). The PCR reaction mixture contained 2.5  $\mu$ L of 10  $\times$  PCR buffer, 0.5  $\mu$ L of 10 pmol each of SSRY13F (5'-CAATGATGGTAAGATGGTGCAG-3') and SSRY13R (5'-GCAAGAATTCCACCAGGAAG-3') primers Mba *et al.* [5], 0.5  $\mu$ L of 10 mM dNTPs, 0.25  $\mu$ L of HotStarTaq DNA Polymerase, and 1  $\mu$ L of 100 ng/ $\mu$ L DNA template. Nuclease-free water was added to achieve a final volume of 25  $\mu$ L. The PCR amplification consisted of 35 cycles including denaturation at 95  $^{\circ}$ C for 45 s, annealing at 60  $^{\circ}$ C for 45 s, and extension at 72  $^{\circ}$ C for 45 s. Before cycling, there was an initial denaturation at 95  $^{\circ}$ C for 5 min, and after cycling, a final extension at 72  $^{\circ}$ C for 5 min was performed using a Thermocycler (Biometra Tone 96, Germany) [5]. The amplified PCR products were separated on 3 % agarose gel in 1  $\times$  TAE buffer and electrophoresed at 120 V for 35 min.

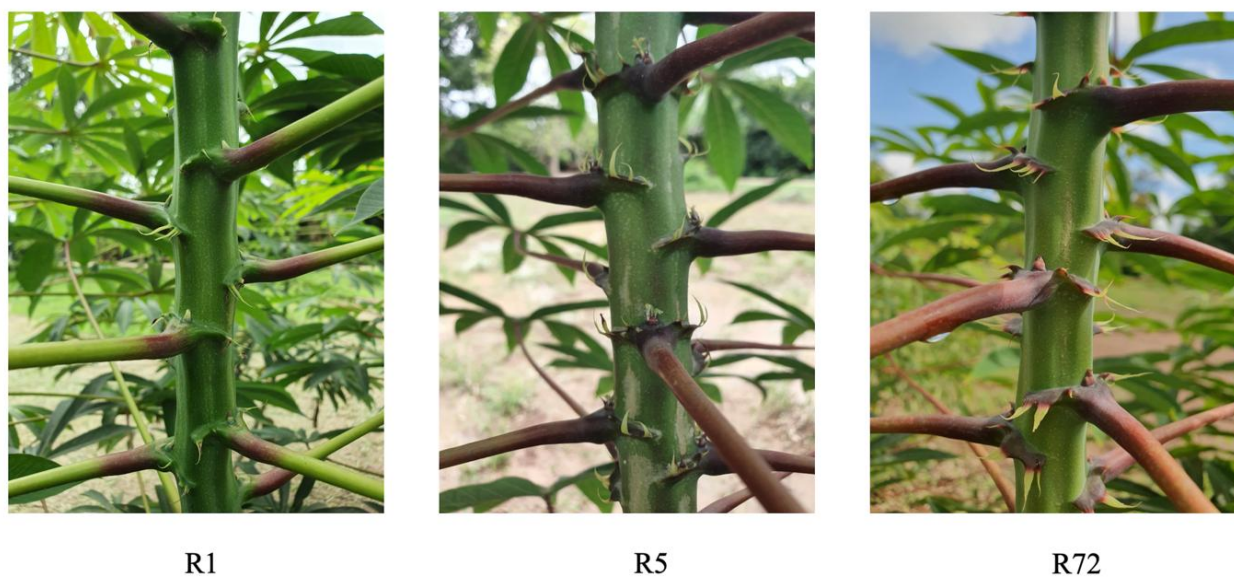


**Figure 2** Cassava cultivars cv R1, cv R5, and cv R72 used in this field study.

### **Identification of cassava hybrids using morphometric analysis**

#### ***Capturing plant photos for analysis***

The photographs were taken outdoors under natural sunlight in standard weather conditions, ensuring consistent lighting across all images. The choice of a 2-m distance allowed for capturing the full spatial extent of the plants while maintaining sufficient detail for analysis. The 180 ° arc was employed to provide a comprehensive spatial representation of the plants and their orientation, accommodating variations in plant structure. To control for variability, all photos were taken with standardized camera settings, including ISO, aperture, and shutter speed. Plant organ images for analysis were chosen by specifically focusing on easily performed components such as leaves and stems. The size of region candidate images was compressed to 224×224 pixels, balancing effective feature extraction and optimizing model performance while minimizing noise from excessive detail. Data for the preliminary analysis included images of cv R1, cv R5, and cv R72 (N=75).

#### ***Data derivatives and multivariate analysis***

The plant organ pictures were analyzed using ImageJ software (version 1.48c, Wayne Rasband, NIH, Bethesda, MD, USA). Color expressions of the cassava leaves and stems were measured using the *histogram order* function, while the degree angles of petioles and

leaf apices were measured using the *angle tool* in ImageJ (Supplementary **Figure S1**). The mean ± standard error values were calculated based on the ImageJ measurements. One-way analysis of variance was used to assess the variability in plant characteristics and the multiple comparison was tested by the Fisher LSD method at significance level 0.05 using Minitab (version 21.4.3, USA). Descriptive statistics were gathered for leaves and stems, and the outcomes were visualized through bar graphs with dot plots. Statistical assumptions were checked for normal distribution and equal variances were assumed for the analysis. Principal component analysis (PCA) was conducted on a dataset exhibiting linear correlations among variables to facilitate the identification of distinct characteristics of the 3 cassava cultivars.

### **Fine-tuning using state-of-the-art architecture for image identity**

#### ***Experimental setup and software***

A Linux Virtual Machine (VM) equipped with the powerful Nvidia A100 GPU was used in our experiments, with leveraging from the PyTorch library Paszke *et al.* [24] for software implementations.

#### ***Training model strategy for discriminating hybrid cassava***

Images of cassava characteristics for identification were also used to fine-tune the deep learning models.

The dataset of 644 images taken by the mobile camera included 3 cassava culture varieties, with each variety R1, R5, and R72 consisting of 74, 444, and 126 images, respectively. This comprehensive fine-tuning study used 4 distinct pretrained models: ResNet-18 He *et al.* [25], AlexNet Krizhevsky *et al.* [26], VGG-16 Simonyan *et al.* [27], and GoogLeNet [28]. The objective was to adapt these models to a specific task by fine-tuning their weights on our target dataset. To ensure robust evaluation, we employed the stratified 3-fold cross-validation approach. The dataset was partitioned into 3 subsets, and in each iteration, 1 subset (33 % of the data) was used as the validation set, while the remaining 2 subsets were used for training. For this dataset of 644 images containing cv R1 (74 images), cv R5 (444 images), and cv R72 (126 images), stratified 3-fold cross-validation maintains the same class proportions in each fold - approximately 11 % for cv R1, 69 % for cv R5, and 20 % for cv R72. This balanced distribution across training and testing sets ensures reliable model evaluation despite the class imbalance, as each fold contains a representative sample of all classes in their original proportions. Each partitioned dataset contained approximately the same percentage of samples of each target class as the complete set (Supplementary **Table S1**).

During the fine-tuning process, we maximized model accuracy, which served as a key performance metric, and used the categorical cross-entropy loss to assess how well the model aligned its predictions with the ground truth labels. Both accuracy and loss provided valuable insights into the model's effectiveness and convergence during training. To ensure a comprehensive evaluation, each experiment was run for a total of 10 epochs. By observing model performance at different stages of training, we assessed how quickly the model converged and whether additional training epochs were required to improve performance. During the fine-tuning process, the data transform played a crucial role in preparing the model input data. The data transform method contained 2 sets of data transformations: One for the training set and the other for the validation set. In the training phase, the process involved several steps. Firstly, the input image underwent random cropping and resizing to achieve dimensions of  $224 \times 224$  pixels, with a 0.5 probability of a horizontal flip being applied to the image.

Subsequently, the image was transformed into a PyTorch tensor, and pixel values were normalized across the RGB color channels. Conversely, during the validation phase, a distinct set of steps was implemented. The input image was resized to  $256 \times 256$  pixels, followed by cropping the central region to obtain dimensions of  $224 \times 224$  pixels. Similar to the training set, the image was then converted into a PyTorch tensor, and pixel values were normalized across the RGB color channels.

By applying these data transformations before the training process, we ensured that the input data were appropriately preprocessed and augmented to enhance model performance and generalization capabilities. The training set benefited from random cropping and flipping for better feature learning, while the validation set underwent resizing and center cropping to ensure uniformity during evaluation. The normalization step was consistent across both datasets to standardize the input features for stable training and reliable predictions.

The Cross-Entropy Loss was chosen as the loss function to optimize model performance. The Stochastic Gradient Descent (SGD) optimizer was employed to update model parameters during training, with a learning rate of 0.001 and a momentum of 0.9. Scheduling the learning rate is a technique that dynamically adjusts the step size at which model parameters are updated during training. It helps to optimize the training process by reducing the learning rate at predefined intervals or based on specific criteria. We used the StepLR scheduler, which multiplies the learning rate by a gamma factor of 0.1 every 5 epochs, ensuring better convergence and performance. By fine-tuning these 4 pretrained models and conducting 3-fold cross-validation with multiple epoch settings, we identified the most suitable model architecture and hyperparameters for our specific task. This rigorous experimentation process enabled us to make informed decisions and deliver a high-performing model with optimal generalization capabilities for our target application.

#### **Evaluation using LIME explanation**

In the evaluation step, after selecting the best-performing fine-tuned model from the 4 pretrained models, we investigated the model decision-making process and its relation to the previous idea of using

morphometric analysis. To achieve this, the local interpretable model-agnostic explanations (LIME) technique was employed to generate interpretable explanations for individual predictions made by the chosen model [22]. The LIME method aims to explain the predicted outcome of a hybrid-cassava image by sampling the images and then generating variants of the image by dividing the image into connected pixels with similar colors. By sorting them, we obtain the parts of the image (superpixels) that have the highest probability for a label. The interpretation of this superpixel image is the part of the (full) image that contributes the most to the prediction.

## Results and discussion

### DNA-based hybrid identification using PCR

DNA amplification using PCR and the separation of DNA fragments via 2 % agarose gel electrophoresis successfully differentiated the 3 cassava cultivars. The presence of DNA fragments in cv R1, cv R5, and cv R72 confirmed the effectiveness of SSRY13 primers for hybrid screening. The PCR products of cv R1 contained a single fragment of approximately 210 bp, while cv R5 had 2 fragments of approximately 220 bp and 190 bp. Similarly, cv R72 exhibited 2 fragments of approximately 220 bp and 210 bp. Notably, both DNA fragments detected in cv R1 and cv R5 were also present in cv R72. These findings demonstrate that SSRY13 primers are effective for hybrid screening in cassava breeding (Supplementary **Figure S2**)

### Morphometric analysis

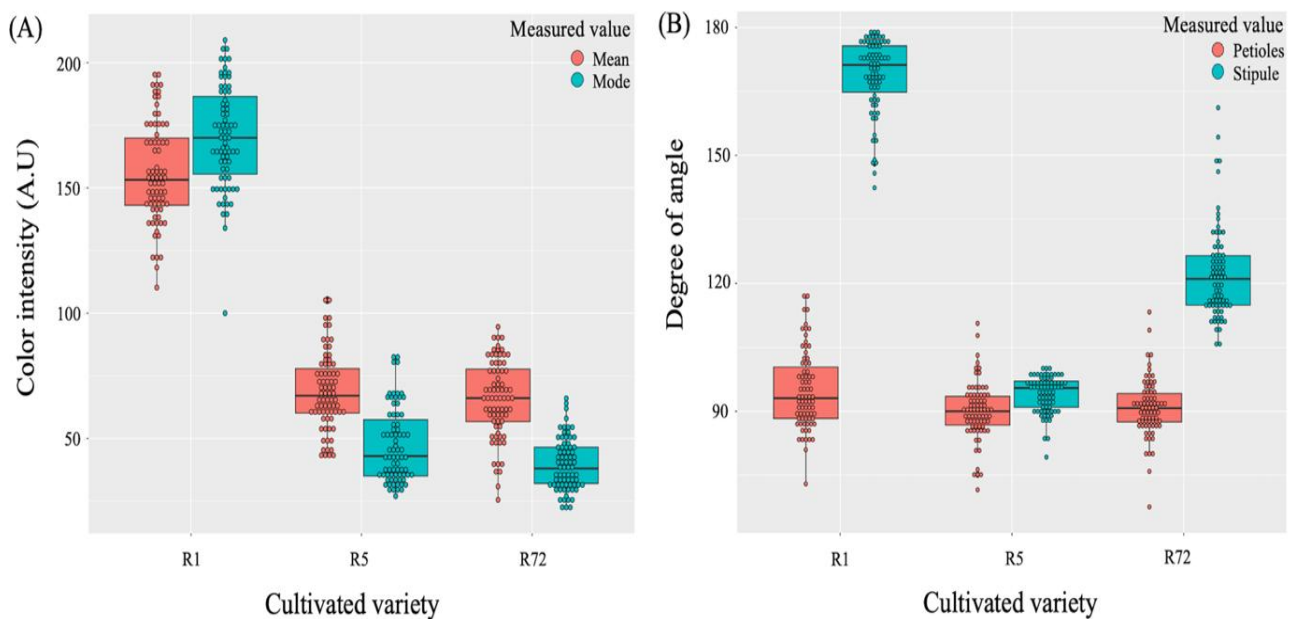
Cassava stem images were selected for measurement using the ImageJ program. A total of 644 photos from the 3 cassava cultivar varieties were subjected to a thorough analysis. As shown in **Table 1**, the ImageJ software was employed to measure the cassava images, focusing on petiole color values in terms of mean (MeP) and mode (MoP) values (**Table 1**). Measurements of the degree angle values between the stem and the petiole (AP) and between the stem and the stipule (AS) were recorded. The MeP and AP values in cv R1 were the highest, and statistically significantly differed from cv R5 and cv R72 ( $p < 0.05$ ), while the

MoP and AS values displayed statistically significant variations among the 3 cultivars ( $p < 0.05$ ). A dot plot (**Figure 3**) was created to visually present the individual data for the 4 distinct characteristics of the 3 cassava cultivar varieties. Correlation among the variables of the 4 cassava characteristics was obtained from the ImageJ measurements. As shown in **Figure 4**, the upper corner displays the correlation coefficient, while the main diagonal represents the distribution of the variables. The results indicated that all variables contribute positively to correlation. Specifically, MeP-MoP and MoP-AS exhibit high R-squared values of 0.97 and 0.86, respectively, indicating strong correlations close to 1. The PCA results of cassava characteristics were used to discriminate cassava hybrids. Specifically, Dim 1 alone accounted for 71.50 % of the variance, and the first 2 dimensions together accounted for up to 94.06 %. However, only one of the 4 principal component axes had an eigenvalue greater than 1. Two characteristics MoP and AS were selected for PCA by considering their statistical significance when tested with ANOVA. The PCA results indicated that 100 % of the total variation could be accounted for by Dim 1 and Dim 2, with Dim 1 explaining up to 92.61 % of the variance. This PCA loaded with MoP and AS shared a significant contribution of 50 % (Supplementary **Figure S3**). The relative discriminating power of PCA as revealed by the eigenvalues was high in Dim 1 at up to 1.85. Thus, we selected the datasets of MoP and AS to create a graphic projection for discriminating the 3 cultivar varieties of cassava. The PCA graphic clearly showed that MoP and AS enabled discrimination between the 3 culture varieties of cassava with  $p$ -values 0.001 (Supplementary **Table S2**). The PCA results demonstrated that the data could be separated into 3 distinct groups. The R1 group was distinctly separated from the R5 and R72 groups (**Figure 5**). In other words, we can identify this cassava by calculating its MoP and AS. However, this method is not practically work in the field as both MoP and AS are difficult to measure accurately in practice. As a result, we developed a deep learning model to assist with this task and verified that the interpretation from the model aligns with those obtained from the PCA.

**Table 1** Morphometric analysis data was quantified utilizing ImageJ software, with PCA conducted using eigenvalues.

Characters	Abbreviation	Morphology measurement			Contributions of variables				Contributions of selected variables	
		cv R1	cv R5	cv R72	Dim 1	Dim 2	Dim 3	Dim 4	Dim 1	Dim 2
Mean of petiole color	MeP	155.95 ± 20.15 <sup>a</sup>	68.75 ± 15.07 <sup>b</sup>	65.67 ± 15.39 <sup>b</sup>	32.47	1.39	22.02	4.41E+01	N/A	N/A
Mode of petiole color	MoP	170.32 ± 20.50 <sup>a</sup>	47.16 ± 14.63 <sup>b</sup>	39.61 ± 10.21 <sup>c</sup>	33.16	1.56	10.22	5.51E+01	50	50
Angle of petiole	AP	94.83 ± 9.09 <sup>a</sup>	90.08 ± 6.82 <sup>b</sup>	90.89 ± 6.78 <sup>b</sup>	5.00	94.93	0.06	1.61E-04	N/A	N/A
Angle of stipule	AS	168.75 ± 8.72 <sup>a</sup>	94.12 ± 4.26 <sup>c</sup>	122.22 ± 10.91 <sup>b</sup>	29.37	2.12	67.69	8.20E-01	50	50
Eigenvalues analysis				Eigenvalue	2.86	0.90	0.21	0.03	1.85	0.15
				Variance%	71.50	22.56	5.20	0.74	92.61	7.39
				Cumulative variance %	71.50	94.06	99.26	100.00	92.61	100.00

Values of morphology measurements are mean ± standard deviation for the 3 cultured varieties of cassava (N = 45). The same lowercase letter within a row indicates no significant statistical difference at  $p < 0.05$  according to the ANOVA test. Eigenvalue analyses were tested for the total amount of variance that could be explained by a given dimension.

**Figure 3** Morphometric analysis of 3 cultivar varieties of cassava, combined with the mean ± standard deviation. The data consists of measurements for stem color intensity (A) and the angles of petioles and stipules (B).

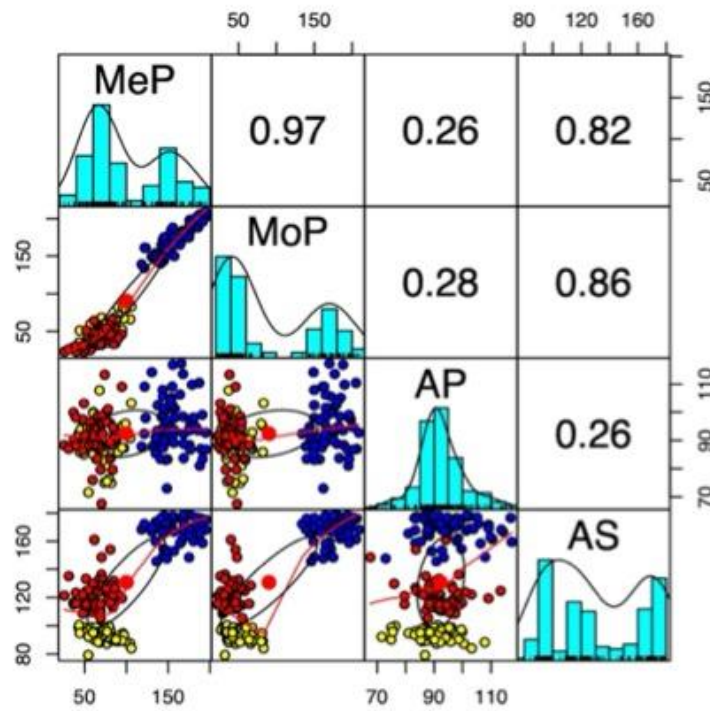


**Figure 4** Correlation analysis between the independent variables. The lower triangles contain scatter plots, while the upper triangles display the corresponding correlation values.

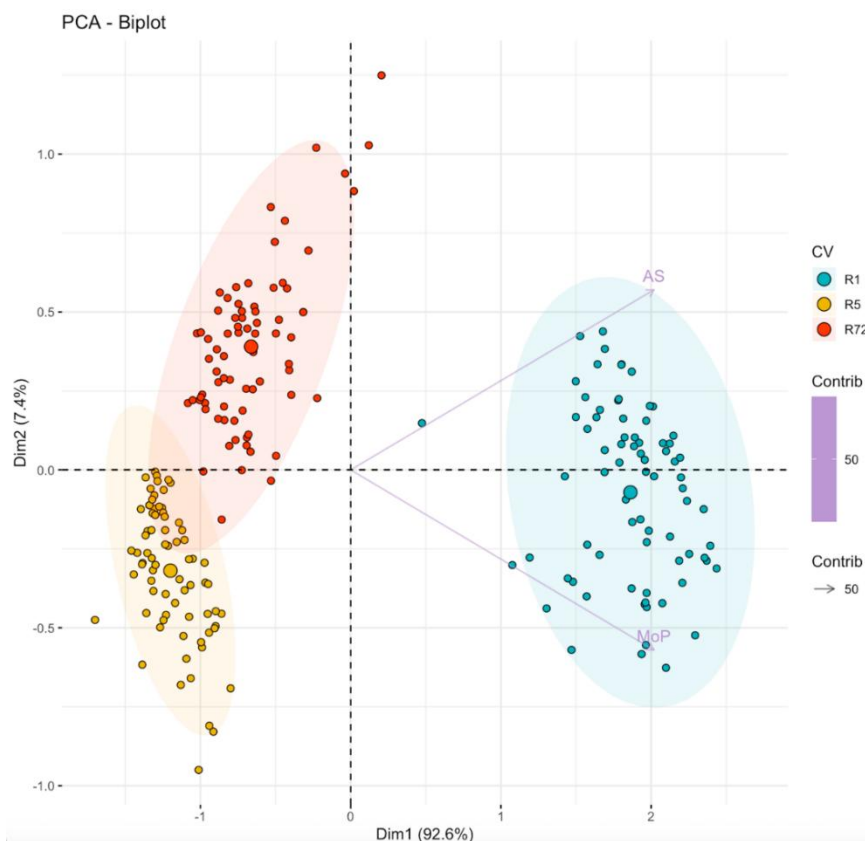


**Figure 5** Principal component analysis (PCA) was performed on 225 data points from Casava cv R1, cv R5, and cv R72 based on mode values of petiole color (MoP) and the degree angle values between the stem and the stipule (AS). The data were used to color individuals by cultivated variety (cv) and variables by their contributions to the principal components using arrows. Dim 1 and Dim 2 explain 92.6 and 7.4 % of the total variation, respectively.

### Comparison of different pretrained models for classifying cassava hybrid images.

The stem region in the cassava images was used to assess the efficacy of the deep neural networks. Principal component analysis (PCA) outcomes were employed to determine the selection of suitable candidate pictures for subsequent machine learning analyses. The 644 images were divided into training and testing datasets as follows: Cv R1 (49 for training and 25 for testing), cv R5 (297 for training and 147 for testing), and cv R72 (85 for training and 41 for testing). The original image size was adjusted to 256x256 pixels, and the region selected for study was cropped to 224x224 pixels to exclude the background. Four convolution network architectures were compared including ResNet-18, VGG-16, AlexNet, and GoogLeNet. The accuracy and categorical cross-entropy loss were utilized to evaluate the performance of these models. Each experiment was conducted for a total of 10 epochs. The choice of 10 epochs was based on empirical observation of the training process. The model showed rapid convergence, reaching near-zero training error in the early epochs, indicating that additional training epochs were unnecessary. Following the fine-tuning process, all models achieved an accuracy surpassing 95 % on the pretrained dataset, except for AlexNet in the 2<sup>nd</sup> fold. ResNet-18 showed the highest percentage of accuracy across all 3 partitions. ResNet-18 was selected for discriminating hybrid cassava because it demonstrated the highest accuracy among the 4 models of 100 % at the 3<sup>rd</sup> fold. The performances of the 4 models were evaluated for accuracy and the estimated training and testing loss (Table 2). Both the

training and testing loss values indicated that the models performed well during both the training and testing phases. The values of training and testing losses remained consistently proximate across all architectures, with a slight increase in testing loss toward the end (Supplementary Figure S4). A confusion matrix was constructed to facilitate a comparative analysis between the predictions and the actual classifications established by the 4 models. As depicted in Table 2, the 4 fine-tuning techniques successfully discriminated among the 3 cassava culture varieties. ResNet-18 achieved the highest accuracy across all 3 folds. However, certain misclassifications were detected within the ResNet-18 results. During both the 1<sup>st</sup> and 2<sup>nd</sup> folds, cv R72 was inaccurately classified as cv R5, while within the 2<sup>nd</sup> fold cv R72 was misidentified as cv R1.

ResNet-18 and GoogLeNet both recorded high accuracy at over 97 % across all 3 folds, with no incorrect predictions in cv R1. The identification of cv R72 gave the highest rate of incorrect predictions among all the architectures (Figure 6). LIME consistently identified specific regions within the same image as significant across multiple explanations, indicating consistent recognition of plant characteristics (Figure 7). LIME confirmed the regions utilized by the model for decision-making and also provided insights into the reasons behind model mispredictions. The visualizations of significant regions' explanations encompass areas with variable colors among the 3 cassava culture varieties, as measured by ImageJ. Results highlighted that the model selected different regions in a manner analogous to the findings of the morphometric analysis study.

**Table 2** Accuracy and loss of training and testing data of execution time at the 10<sup>th</sup> epoch for the 4 models.

Partitions	Metric	Pretrained model			
		ResNet18	VGG-16	AlexNet	GoLeNet
1 <sup>st</sup> fold	accuracy	<b>99.53 %</b>	99.06 %	98.59 %	97.65 %
	train loss	0.1642	0.0527	0.0998	0.2104
	test loss	0.0249	0.0227	0.0432	0.0799
2 <sup>nd</sup> fold	accuracy	<b>99.06 %</b>	96.71 %	94.37 %	98.59 %
	train loss	0.1665	0.1885	0.2323	0.2047
	test loss	0.0381	0.1248	0.1906	0.06
3 <sup>rd</sup> fold	accuracy	<b>100 %</b>	97.65 %	99.06 %	98.59 %
	train loss	0.1662	0.0941	0.1145	0.266
	test loss	0.0197	0.0773	0.0408	0.0518

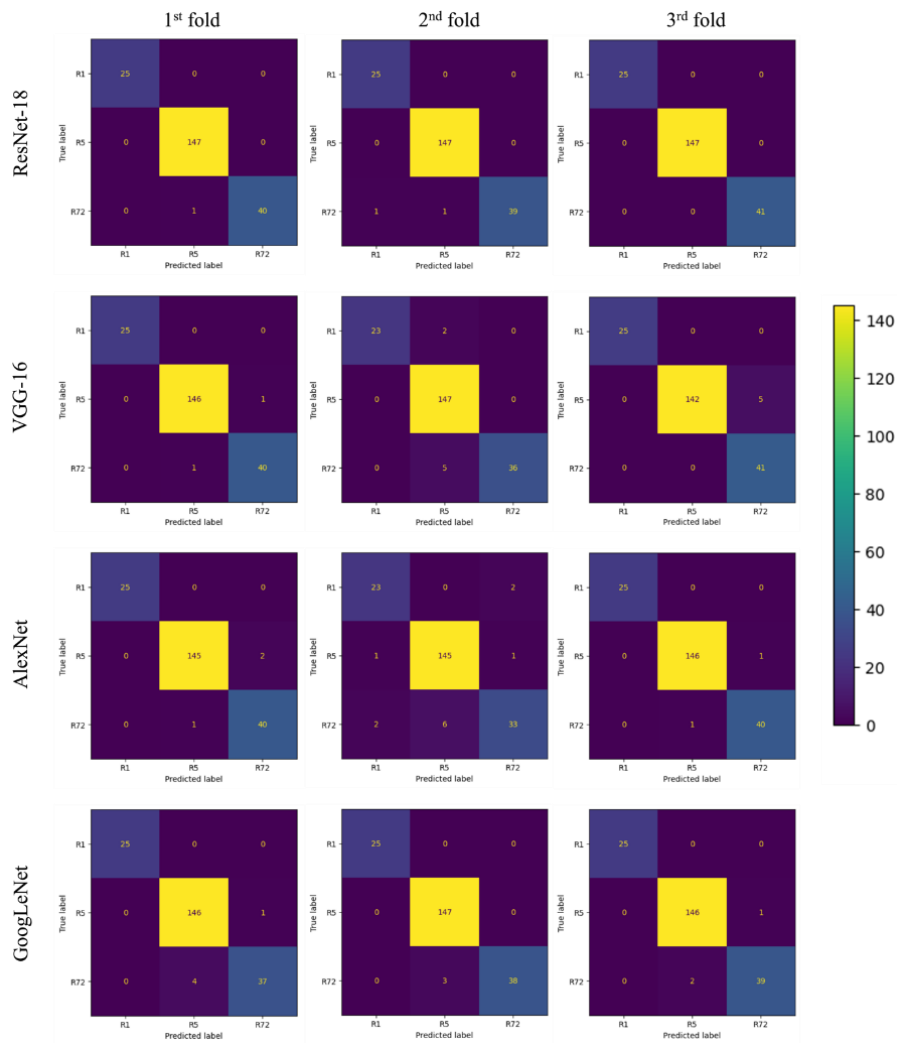


**Figure 6** Confusion matrices obtained from stratified 3-fold cross-validation of the fine-tuning technique. These matrices were generated using the testing dataset and utilized for identifying cassava samples.



**Figure 7** Elucidate a prediction using LIME from the ResNet-18 architecture model, artificial data is generated from the original image through subsets created using LIME. Artificial data were created from the original image subsets using LIME to evaluate which part of the image the model made its decision.

## Discussion

Many cassava cultivars can be distinguished based on biological characteristics including tuber and leaf shape, productivity, and the percentage of cyanogenic glycosides [29]. Identifying cassava varieties can be challenging due to the close resemblance of their external morphology. Identification of cassava varieties is now conducted using a combination of morphological analysis and molecular techniques, specifically PCR-based methods using various molecular markers including PCR-RFLP (Restriction Fragment Length Polymorphisms), PCR-RAPD (Random Amplified Polymorphic DNAs), PCR-AFLP (Amplified Fragment Length Polymorphisms), SNP (Single-Nucleotide Polymorphisms), and Simple Sequence Repeats (SSR) [6,30]. SSR markers are popular for the identification of cassava varieties that are used for the development of hybrid cassava varieties such as cv R1 and cv R5 [31]. However, despite showing potential for identifying cassava varieties, these processes still necessitate the use of sophisticated equipment and require many steps for DNA amplification and product analysis [31]. The conventional method relies on morphometric analysis, requiring the involvement of expertise or taxonomists, and is not suitable for application on a large scale. In this study, we solved 2 key challenges for identifying cassava varieties on a large scale by using machine learning. Numerous studies have been conducted utilizing plants as samples to investigate plant diseases or to identify plant species [12,32,33]. However, previous studies did not include the identification of hybrid plants and mainly focused on the results obtained from machine learning investigations. Therefore, we used computer vision techniques with machine learning to identify the varieties of cassava, based on the results of morphometric analysis. This method is reliable and can be applied to other plants. It enables identification based on leaves and stems, avoiding the reliance on flowers that are seasonally limited.

PCA was used to visually represent and analyze 3 cassava varieties based on the data collected through ImageJ. PCA is commonly used in the field of data processing for dimensionality reduction. Images of the region between the stem and leaves were used in this study due to their numerous amounts and simplicity for use in field investigations. Data were obtained from 4

characteristics seen in this image region. Statistical analysis of the findings was conducted using the Mann-Whitney U test, with results statistically different at  $p$ -value  $< 0.05$  selected and used for PCA. ImageJ software was used to measure the cassava stem images, focusing on petiole color and angle values between the stem and petiole and stipule. Analysis of the 3 cassava cultivar varieties revealed significant differences in mean petiole color and angle values. Visual representation through dot plots highlighted individual data for the characteristics of the cultivar varieties. Correlation analysis indicated strong positive correlations among variables, particularly between mean and mode petiole color and mode and stipule angle. Principal component analysis (PCA) further discriminated cassava hybrids based on measured characteristics, with the first 2 dimensions explaining the majority of variability. Notably, the PCA loaded with mode petiole color and stipule angle contributed significantly to discriminating cultivar varieties, with the analysis explaining 100 % of the total variance. Graphic projections based on the PCA results confirmed the effective discrimination of the 3 cassava cultivar varieties, with distinct separation of the R1 group from the R5 and R72 groups. These findings underscored the utility of ImageJ-based measurements and PCA in characterizing and discriminating cassava cultivar varieties based on morphological traits. In particular, if the eigenvalue of a principal component was almost equal to 1 and the cumulative contribution rate was above or equal to 85 %, the corresponding data were deemed suitable for consideration and further analysis [34]. Wang *et al.* [35] also noted that the significance of PCA can potentially reduce the dimensions of the data while preserving all the information. This reduction in dimensionality may lead to a decrease in the number of neurons in the input layer, resulting in enhanced speed of the neural networks. The outcome was achieved using PCA and neural networks for plant disease detection, demonstrating accuracy and prediction accuracy of up to 100 % [35]. However, PCA was not suitable for handling non-linear data. Other techniques are required if the extracted features are non-linear data, which is often the case with data obtained from natural samples [34,35].

Various studies have successfully applied machine learning for plant sample identification and also for plant disease investigation. Sun *et al.* [36] showed that the ResNet-26 model identified up to 100 plant species with an accuracy of 91.78 % in the test dataset Sun *et al.* [36], while Grinblat *et al.* [37] examined a CNN model for plant identification based on leaf vein patterns. Results indicated that the standard deep learning model showed the potential to enhance the accuracy of plant identification based on leaf patterns [37]. Similarly, other studies have achieved successful plant identification using only 1 plant characteristic such as leaf [19,21], flower [18], and fruit [38]. Previous studies suggested that deep learning models can only use 1 plant characteristic for plant identification. This benefit may be useful for applications in the field and in industry for automated classification on a large scale [38,39]. This study compared 4 fine-tuning models to identify 3 varieties of cassava. Findings indicated that ResNet-18 achieved maximum accuracy of 100 %, whereas the other techniques achieved accuracies of up to 94 % when applied to our dataset. The experimental results demonstrated that using any method for training and testing with our dataset gave a high level of accuracy. Deep learning has demonstrated exceptional performance considering the number of parameters and time for training compared to the state-of-the-art [12,17,19]. Due to the high accuracy achieved, this method may be acceptable for any state-of-the-art study. When compared to conventional techniques, our approach demonstrated higher accuracy, was easier to perform, and did not need expertise. Nevertheless, 1 point that needs answering is what aspect of the image was employed to investigate the separation of the 3 cassava varieties because machine learning methods are “black-box”. It was a research gap since it is hard for humans to understand which such model used and gave accurate predictions. In this study, we will answer the question by implement the result from morphometric analysis and using LIME was used not only to see the specific region of an image that the model utilized, but it also has the capability to elucidate the regions that contribute to misclassification. LIME confirmed that the area shown in the image corresponded to the identical region used in our previous PCA. Four characteristics that we used in PCA could be observed from the region where the LIME result was observed. However, we do

not claim that models used 4 data to identify the cassava variety because these results only explain the observed correlation of the region for identifying 3 cassava varieties. Most misclassifications in the model were attributed to the use of image aspects that were far from the stem and petiole such as leaves from other plants growing nearby and captured in the same image. This may provide valuable insights about the development of a technique aimed at improving accuracy, and address the limitations associated with capturing photographs during field studies. Numerous studies have used LIME for type selection to give the best performance Togacar *et al.* [40] or improved model prediction interpretability [41]. Our results confirmed the effectiveness of LIME as a crucial tool for facilitating the examination of datasets subjected to deep learning analysis. LIME can be used to enhance the interpretability and transparency of complex deep learning models, thereby enabling researchers to gain deeper insights into the underlying mechanisms and decision-making processes of these models. The result of this study highlighted the practical applications of LIME for validating the results of deep learning analyses compared with data from measurements.

## Conclusions

In the present study, ResNet-18 showed promising potential by accurately identifying the 3 cassava varieties, with accuracy of 100 % in the 3rd fold. LIME validated that the area shown in the image corresponded to the same region used in our result from PCA. This information may be utilized to develop a model with improved accuracy or further develop a mobile application based on our datasets. All the findings emphasized the need to establish a strategy for future identification of plants with similar genetic varieties, which can be utilized successfully in large-scale field studies.

## Acknowledgements

This work was supported by Faculty of Science, Naresuan University, Thailand (grant number is R2565E027). Our computational resources and software were provided by the Department of Mathematics, Faculty of Science, Naresuan University, Thailand.

## References

- [1] A Bellotti, BVH Campo and G Hyman. Cassava production and pest management: Present and potential threats in a changing environment. *Tropical Plant Biology* 2012; **5**, 39-72.
- [2] P Kongsil, H Ceballos, W Siriwan, S Vuttipongchaikij, P Kittipadakul, C Phumichai, W Wannarat, W Kositratana, V Vchukit, E Sarobol and C Rojanaridpiched. Cassava breeding and cultivation challenges in thailand: Past, present, and future perspectives. *Plants* 2024; **13(14)**, 1899.
- [3] EJD Oliveira, SASD Oliveira, SAV Boas, CS Hohenfeld and VDS Santos. Selection of cassava accessions with multiple resistance to pathogens associated with root rot disease. *Euphytica* 2017; **213**, 185.
- [4] P Changtor, W Jaroenpol, K Buddhachat, W Wattanachaiyingcharoen and N Yimtragool. Rapid detection of *Sclerotium rolfsii* causing dry stem and root rot disease in cassava by recombinase polymerase amplification technique (RPA) combined with CRISPR/Cas12a. *Crop Protection* 2023; **172**, 106340.
- [5] REC Mba, P Stephenson, K Edwards, S Melzer, J Nkumbira, U Gullberg, K Apel, M Gale, J Tohme and M Fregene. Simple sequence repeat (SSR) markers survey of the cassava (*Manihot esculenta* Crantz) genome: Towards an SSR-based molecular genetic map of cassava. *Theoretical and Applied Genetics* 2001; **102**, 21-31.
- [6] J Adjebeng-Danquah, J Manu-Aduening, IK Asante, RY Agyare, V Gracen and SK Offei. Genetic diversity and population structure analysis of Ghanaian and exotic cassava accessions using simple sequence repeat (SSR) markers. *Heliyon* 2020; **6(1)**, e03154.
- [7] D Nadjiam, P Sarr, M Naitormbaide, M Mbailao and A Guisse. Agro-morphological characterization of cassava (*Manihot esculenta* Crantz) cultivars from chad. *Agricultural Sciences* 2016; **7(7)**, 479-492.
- [8] Z Li, R Guo, M Li, Y Chen and G Li. A review of computer vision technologies for plant phenotyping. *Computers and Electronics in Agriculture* 2020; **176**, 105672.
- [9] K Suzuki. Overview of deep learning in medical imaging. *Radiological Physics and Technology* 2017; **10(3)**, 257-273.
- [10] Z Zhao, P Zheng, S Xu and X Wu. Object detection with deep learning: A review. *IEEE Transactions on Neural Networks and Learning Systems* 2019; **30(11)**, 3212-3232.
- [11] I Adjabi, A Ouahabi, A Benzaoui and A Taleb-Ahmed. Past, present, and future of face Recognition: A review. *Electronics* 2020; **9(8)**, 1188.
- [12] EC Too, L Yujian, S Njuki and L Yingchun. A comparative study of fine-tuning deep learning models for plant disease identification. *Computers and Electronics in Agriculture* 2019; **161**, 272-279.
- [13] M Torky, G Dahy and AE Hassanien. Recognizing sounds of Red Palm Weevils (RPW) based on the VGGish model: Transfer learning methodology. *Computers and Electronics in Agriculture* 2023; **212**, 108079.
- [14] X Jin, J Xiong, Y Rao, T Zhang, W Ba, S Gu, X Zhang and J Lu. TranNas-NirCR: A method for improving the diagnosis of asymptomatic wheat scab with transfer learning and neural architecture search. *Computers and Electronics in Agriculture* 2023; **213**, 108271.
- [15] I Khan, SS Sohail, DO Madsen and BK Khare. Deep transfer learning for fine-grained maize leaf disease classification. *Journal of Agriculture and Food Research* 2024; **16**, 101148.
- [16] KK Saha, A Rahman, M Moniruzzaman, M Syduzzaman, MZ Uddin, MM Rahman, MA Ali, DFA Riza and MMH Olivar. Classification of starfruit maturity using smartphone-image and multivariate analysis. *Journal of Agriculture and Food Research* 2023; **11**, 100473.
- [17] MM Ghazi, B Yanikoglu and E Aptoula. Plant identification using deep neural networks via optimization of transfer learning parameters. *Neurocomputing* 2017; **235**, 228-235.
- [18] T Nguyen, TL Le, H Vu, H Nguyen and HV Sam. *A combination of deep learning and hand-designed feature for plant identification based on leaf and flower images*. Springer Nature, London, 2017.

- [19] P Jasitha, MR Dileep and M Divya. Venation based plant leaves classification using GoogLeNet and VGG. *In: Proceedings of the 4<sup>th</sup> International Conference on Recent Trends on Electronics, Information, Communication & Technology (RTEICT), Bangalore, India. 2019.*
- [20] O J V Ramirez, JECDI Cruz and WAM Machaca. Agroindustrial plant for the classification of hass avocados in real-time with ResNet-18 architecture. *In: Proceedings of the 5<sup>th</sup> International Conference on Robotics and Automation Sciences (ICRAS), Wuhan, China. 2021.*
- [21] SY Arafat, N Arshad and R Khan. Holistic based plant identification using deep learning. *In: Proceedings of the 16<sup>th</sup> International Conference on Emerging Technologies (ICET), Islamabad, Pakistan. 2021.*
- [22] MT Ribeiro, S Singh and C Guestrin. "Why should i trust you?": Explaining the predictions of any classifier. *In: Proceedings of the 22<sup>nd</sup> ACM SIGKDD International Conference on Knowledge Discovery and Data Mining, California. 2016.*
- [23] K Sharma, R Bhattacharjee, A Sartie and P Kumar. An improved method of DNA extraction from plants for pathogen detection and genotyping by polymerase chain reaction. *African Journal of Biotechnology* 2013; **12(15)**, 1894-1901.
- [24] A Paszke, S Gross, F Massa, A Lerer, J Bradbury, G Chanan, T Killeen, Z Lin, N Gimelshein, L Antiga, A Desmaison, A Köpf, E Yang, Z DeVito, M Raison, A Tejani, S Chilamkurthy, B Steiner, L Fang, ..., S Chintala. *In: Proceedings of the 33<sup>rd</sup> International Conference on Neural Information Processing Systems, New York. 2019, p. 8026-8037.*
- [25] K He, X Zhang, S Ren and J Sun. Deep residual learning for image recognition. *In: Proceedings of the IEEE conference on computer vision and pattern recognition, Nevada. 2016.*
- [26] A Krizhevsky, I Sutskever and GE Hinton. ImageNet classification with deep convolutional neural networks. *Communications of the ACM* 2017; **60(6)**, 84-90.
- [27] K Simonyan and A Zisserman. *Very deep convolutional networks for large-scale image recognition.* International Conference on Learning Representations, California, 2015.
- [28] C Szegedy, W Liu, Y Jia, P Sermanet, S Reed, D Anguelov, D Erhan, V Vanhoucke and A Rabinovich. Going deeper with convolutions. *In: Proceedings of the IEEE conference on computer vision and pattern recognition 2014, Ohio. 2014.*
- [29] SK O'Hair. Tropical root and tuber crop. *Horticultural Reviews* 1990; **12**, 157-196.
- [30] S Sivan, K Arya, MN Sheela, BS Revathi, BSP Krishnan and SK Muthusamy. Genetic diversity analysis of Indian Cassava (*Manihot esculenta* Crantz) accessions using morphological and molecular markers. *South African Journal of Botany* 2023; **161**, 347-357.
- [31] S Ngorian, J Kansup, B Ruangwiset, V Chanroj, S Amawan and P Wongtiem, The study of genetic diversity of cassava (*Manihot esculenta*) using SSR markers. *Thai Agricultural Research Journal* 2019; **37(1)**, 2-13.
- [32] A Kaya, AS Keceli, C Catal, HY Yalic, H Temucin and B Tekinerdogan. Analysis of transfer learning for deep neural network-based plant classification models. *Computers and Electronics in Agriculture* 2019; **158**, 20-29.
- [33] Y Chen, Y Huang, Z Zhang, Z Wang, B Liu, C Liu, C Huang, S Dong, X Pu, F Wan, X Qiao and W Qian. Plant image recognition with deep learning: A review. *Computers and Electronics in Agriculture* 2023; **212**, 108072.
- [34] F Jia, EB Martin and A J Morris. Non-linear principal components analysis for process fault detection. *Computers & Chemical Engineering* 1998; **229(1)**, 851-854.
- [35] H Wang, G Li, Z Ma and X. Li. Image recognition of plant diseases based on principal component analysis and neural networks. *In: Proceedings of the 8<sup>th</sup> International Conference on Natural Computation, Sichuan. 2012.*
- [36] Y Sun, Y Liu, G Wang and H Zhang. Deep learning for plant identification in natural environment. *Computational Intelligence and Neuroscience* 2017; **2017(1)**, 7361042.
- [37] GL Grinblat, LC Uzal, MG Larese and PM Granitto. Deep learning for plant identification using vein morphological patterns. *Computers and Electronics in Agriculture* 2016; **127**, 418-424.

- [38] MS Hossain, M Al-Hammadi and G Muhammad. Automatic fruit classification using deep learning for industrial applications. *IEEE Transactions on Industrial Informatics* 2019; **15(2)**, 1027-1034.
- [39] A Rocha, DC Hauagge, J Wainer and S Goldenstein. Automatic fruit and vegetable classification from images. *Computers and Electronics in Agriculture* 2010; **70(1)**, 96-104.
- [40] M Togaçar, N Muzoglu, B Ergen, BSB Yarman and AM Halefoglu. Detection of COVID-19 findings by the local interpretable model-agnostic explanations method of types-based activations extracted from CNNs. *Biomedical Signal Processing and Control* 2022; **71**, 103128.
- [41] X Zhao, L Zhang, G Zhu, C Cheng, J He, S Traore and VP Singh. Exploring interpretable and non-interpretable machine learning models for estimating winter wheat evapotranspiration using particle swarm optimization with limited climatic data. *Computers and Electronics in Agriculture* 2023; **212**, 108140.

### Supplementary material

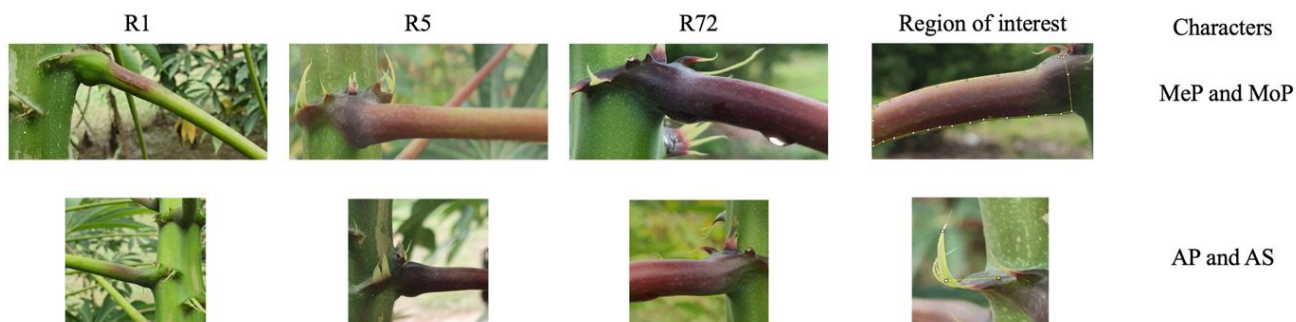


**Figure S1** The region of the plant organ pictures was analyzed using ImageJ software.

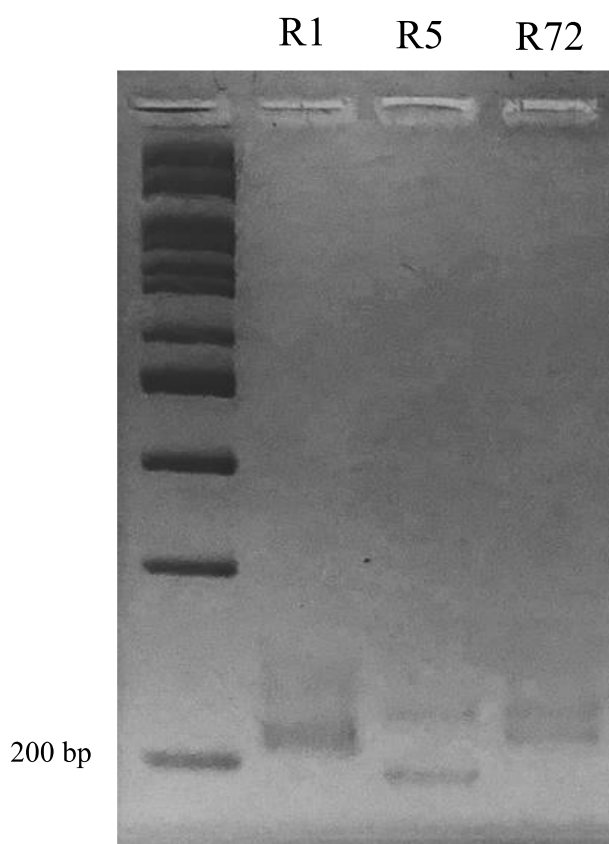


**Figure S2** The PCR amplification results with SSRY13 primer show that the PCR product of R1 has 1 fragment, whereas R5 and R72 exhibit two fragments.

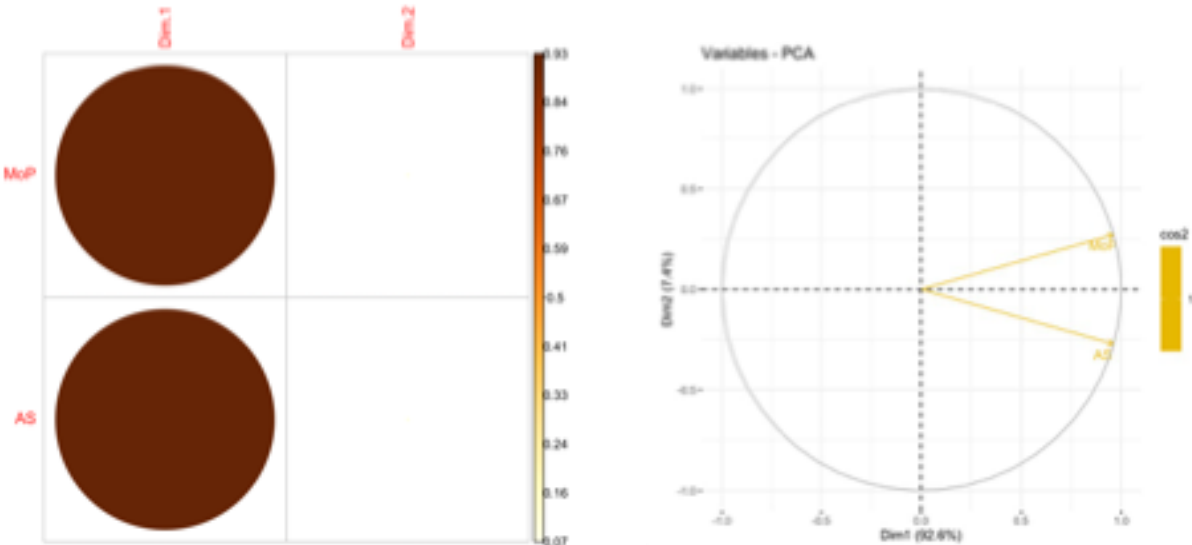
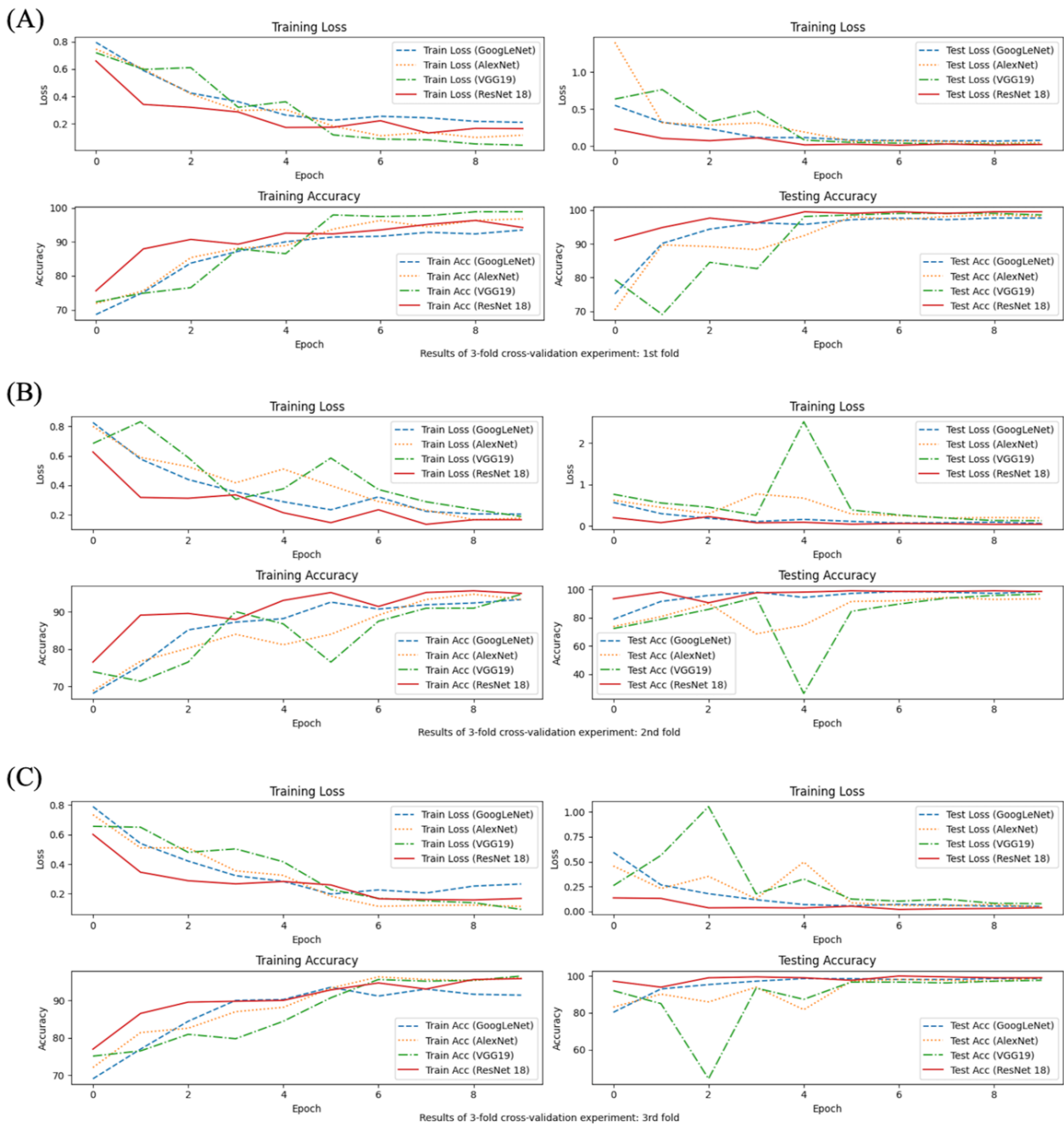


Figure S3 The PCA loadings illustrate the relative contributions of MoP and AS to Dimension 1.



**Figure S4** Accuracy and loss for training and testing ResNet-18 with 3 replications (A) - (C) were evaluated.

**Table S1** Data separation strategies for fine-tuning study.

1st fold			213
2nd fold		213	
3rd fold	213		

Green is the validation set; Orange is the training set.

**Table S2** P-Values for principal components.

	<b>df</b>	<b>Sum of Sqs</b>	<b>R<sup>2</sup></b>	<b>F</b>	<b>Pr (&gt;F)</b>
Model	2	1020867	0.93545	1608.5	0.001***
Residual	222	70449	0.06455		
Total	224	1091316	1.000		